Journal of Hazardous Materials 487 (2025) 137195

Contents lists available at ScienceDirect

Journal of Hazardous Materials

journal homepage: www.elsevier.com/locate/jhazmat

Targeted and non-targeted metabolic analysis of chlorpromazine in grass carp as well as the *in-silico* and metabolomics toxicity assessment

Jinxia Dai [a], Sen Zhang [a], Hui Lin [b], Jun-qin Qiao [a], Hong-zhen Lian [a,*], Chun-xiang Xu [b,**]

[a] State Key Laboratory of Analytical Chemistry for Life Science, School of Chemistry & Chemical Engineering and Center of Materials Analysis, Nanjing University, Nanjing 210023, China
[b] Jiangsu Institute for Food and Drug Control, 6 Beijing West Road, Nanjing 210008, China

HIGHLIGHTS

- Thirteen CPZ metabolites were identified, including 2 newly identified metabolites.
- The structures and transformation pathways of CPZ metabolites in fish were deduced.
- The ecotoxicity of CPZ and its metabolites was estimated by toxicity prediction.
- CPZ exposure could cause metabolic disorder in the endogenous metabolome of fish.

GRAPHICAL ABSTRACT

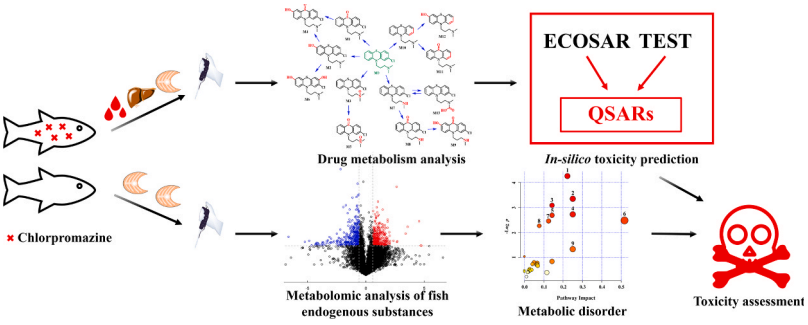

ARTICLE INFO

Keywords:
Chlorpromazine
Grass carp
Metabolite
Toxicity prediction
Metabolomics

ABSTRACT

Chlorpromazine (CPZ) is an abused sedative that is extensively metabolized in organisms. However, the metabolic pathway of CPZ in aquatic organisms is still unclear. In this study, CPZ metabolites was analyzed in grass carp exposed to CPZ in the raising water using ultrahigh-performance liquid chromatography coupled with quadrupole Orbitrap mass spectrometry (UHPLC-Q-Orbitrap MS). Thirteen CPZ metabolites were identified, including 11 previously reported and 2 newly identified metabolites (M9 and M13), and 5 known metabolites were confirmed using authentic standards. The molecular structures and transformation pathways of CPZ metabolites were putatively deduced, which mainly included oxygenation, demethylation, dechlorination and carboxylation reactions. Quantitative analysis of CPZ and its metabolites were also performed, and CPZ sulfoxide had a higher content as an important characteristic metabolite. In addition, *in-silico* toxicity prediction reminded that some metabolites possess ecotoxicity and developmental toxicities similar to, or even higher, than CPZ. Moreover, metabolomics results indicated that CPZ exposure could cause metabolic disorder in the endogenous metabolome of grass carp.

* Correspondence to: School of Chemistry & Chemical Engineering and Center of Materials Analysis, Nanjing University, 163 Xianlin Avenue, Nanjing 210023, China.
** Corresponding author.
E-mail addresses: hzlian@nju.edu.cn (H.-z. Lian), xcx70@163.com (C.-x. Xu).

https://doi.org/10.1016/j.jhazmat.2025.137195
Received 3 October 2024; Received in revised form 2 January 2025; Accepted 11 January 2025
Available online 12 January 2025

1. Introduction

Aquatic products are one of the important food types, and the related food safety issues are closely related to human health. In aquaculture, drugs such as anesthetics and sedatives targeting the nervous system are often used to prevent damage during transportation apart from the cure of animal diseases, such as chlorpromazine (CPZ), azaperone, diazepam, estazolam, haloperidol, nitrazepam, oxazepam, and perphenazine [1]. However, excessive exposure or abuse of these drugs contaminates water and results in drug residues in aquatic species, which could affect fish health and quality of aquatic ecosystems. In addition, anesthetic and sedative residues in environmental waters have been reported to adversely affect fish and have been detected in fish [2–4]. These drugs will be transformed into various products with unknown toxicity under the action of environment, microorganisms, fish and other factors, some of which are still relatively toxic. The drug residues are likely to bioaccumulate through the food chain and are potentially dangerous to humans. Therefore, various countries and international organizations have prescribed strict restrictions for these drugs in edible fish. However, the coverage of compounds in the targeted analysis method of the current commonly used liquid chromatography tandem mass spectrometry (LC-MS/MS) is limited, ignoring the unknown risk compounds. To solve this problem, non-targeted screening methods are needed to comprehensively analyze the known and unknown compounds in fish.

CPZ as a sedative is a representative phenothiazine derivative for the treatment of psychiatric disease and is one of the four anti-psychiatric drugs on the basic medical list of the World Health Organization (WHO). CPZ is also a veterinary medicine used for sedation, hypnosis, anesthesia, antiemetic and weight gain. Furthermore, CPZ also reduces stress response in animals and decreases mortality during long-distance delivery [5]. However, the overdose of CPZ intake may cause kidney damage, liver damage, and cardiac injury in humans [6–8]. Therefore, the European Union prohibits the use of CPZ in edible animals [9], while Japan and China require that it should not be detected in foodstuffs of animal origin [10,11]. The official standard methods for specifically analyzing CPZ in fishery products based on LC-MS/MS were issued both in Japan [12] and China [13]. Nonetheless, CPZ residues are frequently detected in aquatic animals and/or in environmental waters [4]. Studies have found that CPZ has been detected in the Henares-Jarama-Tajo River (Madrid, Spain) [14], surface water and treated sewage (London, England) [15], psychiatric hospital wastewater (Beijing, China) [16], and wastewater from the University Hospital of the Federal University of Santa Maria (Rio Grande do Sul, Brazil) [17] at concentrations ranging from 0.001 to 0.52 μg L^{-1}, and especially in aquatic invertebrates collected from streams in Melbourne, Australia [18], at approximately 50 μg kg^{-1}.

It is a remarkable fact that CPZ is extensively metabolized into a variety of metabolites *in vivo*. Theoretically there may be as many as 168 human metabolites [19], and it can be converted into various degradation products under the influence of the environment [20,21]. Nishimura et al. studied the metabolism of CPZ in rats and speculated that CPZ in rat plasma is mainly converted into CPZ sulfoxide (CPZSO), CPZ-N-oxide (NOCPZ), desmethyl CPZ (DMCPZ) and didesmethyl CPZ (DDMCPZ) [22]. Jiménez et al. explored the fate of CPZ in river water, and 16 degradation products of CPZ were detected [20]. Trautwein et al. investigated the degradation of CPZ under environmental conditions. They found a total of 61 abiotic and biotransformation products but only elucidated the molecular structures of 3 aerobic and 1 anaerobic biotransformation products, and found a total of 57 photolysis products but only elucidated the molecular structures of the main three photolysis products [21]. Most of the conversion products of CPZ retain the phenothiazine group, such as CPZSO, 7-hydroxychlorpromazine (7-HOCPZ), NOCPZ, DMCPZ and so on. It has also been reported that during the metabolism of CPZ in the human body, less than 1 % of the original CPZ drug and 20–70 % in the form of metabolites are excreted in urine, and 5–6 % are excreted in feces [23]. Very importantly, previous researches have shown that partial metabolites or degradation products of CPZ have longer residual periods and higher toxicity than the parent drug [20,24,25].

Aquatic species are affected by drug abuse and the residue in environmental waters. Although there are some reports on the metabolism of CPZ in the existing literature, they are mainly focused on humans and other animals such as rats, and are all relatively early studies. To the best of our knowledge, however, there have been no reports on the metabolism of CPZ in aquatic species so far. Therefore, it is necessary to carry out targeted and non-targeted drug metabolism studies in edible fish for CPZ, in order to screen and identify CPZ metabolites and elucidate the drug metabolic mechanism of CPZ in fish. Our laboratory has previously established a qualitative and quantitative method for CPZ and its four metabolites CPZSO, 7-HOCPZ, DMCPZ and promazine (PZ) in fish, pork, beef and mutton samples using ultrahigh-performance liquid chromatography coupled with quadrupole Orbitrap mass spectrometry (UHPLC-Q-Orbitrap MS) [26], however, the *in-vivo* metabolism of CPZ in these animal-derived foods was not investigated. The aim of this present work is to identify more metabolites in fish, elucidate the metabolic pathways of CPZ, conduct accurate quantitative and semi-quantitative analyzes of CPZ and its metabolites, find out the metabolic patterns, screen out representative metabolites. The toxicity risk of CPZ and its metabolites is preliminary estimated through toxicity prediction software. Additionally, non-targeted metabolomic analysis is performed to explore the effect of CPZ exposure on the metabolome of grass carp.

2. Materials and methods

The chemical, reagents and instrument conditions used in this work were provided in detail in the Supporting Information.

2.1. Animal experiments

Grass carp (*Ctenopharyngodon idella*) was selected as the experimental animal because it is a widely farmed food fish. This study complied with the Chinese legislation and was approved by the independent animal ethics committee of Nanjing University, and performed in accordance with the guidelines for care and use of Nanjing University. Fifty healthy grass carp (10 ± 1 cm, 15 ± 2 g, 3 months old) were purchased from Linghu freshwater fish production base (Huzhou, China) and were transported in four fish tanks (Long × Width × Height: 39 cm × 27 cm × 44 cm) in the micro-flowing water purification system with a photoperiod of 14 h/10 h (light/dark). The fish tank used a filter device to circulate water in and out, forming a self-circulation and continuous oxygenation. The filter device was a physical filter composed of gauze filter cotton, volcanic stone, medical stone, etc., in order to remove impurities and microorganisms in the water and protect the fish. Tap water exposed to the sun light for a day was used for fish farming to remove chlorine from the water. The fish feed was directly thrown into the water through the feeding hole, with feeding occurring once a day. Considering the safety issues of fish exposed to CPZ and the mass spectrometry signal response intensity of CPZ and its metabolites, and referring to the recommended dosages of other animals according to the medication instructions of CPZ hydrochloride injection (Jilin Huamu Animal Health Products Co., Ltd., Jilin, China), the CPZ exposure concentration of 0.5 mg L^{-1} was proposed. After feeding for 5 days, CPZ was added to the water at a concentration of 0.5 mg L^{-1}, and clean water was restored after 24 h. On the 1st, 2nd, 4th, and 7th day, two fish samples were selected from the drug treatment group and the control group respectively for metabolism research of CPZ. The skin surface of the fish was rinsed with phosphate buffer saline (PBS) buffer. Fish blood was collected by cutting tail after the fish was dazed by slapping its head. Serum was obtained by centrifugation of blood at 16,900 g for 10 min, and the liver and muscle tissues were quickly frozen in liquid nitrogen after dissection. All samples were stored at −80 °C until analysis. After

the samples were thawed, a certain volume of serum samples was directly taken for further sample preparation. Liver samples were vortexed, and muscle samples were homogenized with a blender, and then weighed separately for further sample preparation. In addition, six fish samples were selected in each of the two groups for metabolomic analysis of endogenous substances in fish muscle on the 4th day.

2.2. Sample preparation

For drug metabolism analysis, aliquots of 20 μL of mixed serum or 40 mg of mixed liver or 100 mg of mixed muscle samples were thawed on ice, and 10 μL of internal standard solution CPZ-D6 at 100 μg L^{-1} was mixed with samples. The mixture was vortexed for 30 s and then stood in the dark for 10 min. After being added acetonitrile saturated with n-hexane (1 mL for serum sample, 2 mL for liver sample and 5 mL for muscle sample), the sample was vortexed for 1 min, ultrasonically extracted for 10 min and then centrifuged at 16,900 g for 5 min. The supernatant was transferred into an appropriate volume centrifuge tube and was dried in a nitrogen blower. The residue was reconstituted with 200 μL of acetonitrile, then vortexed for 30 s, and filtered through 0.22 μm organic phase membrane filters for UHPLC-Q-Orbitrap MS analysis.

For metabolomic analysis of fish endogenous substances, 100 mg of fish muscle tissues were weighed into a 2 mL centrifuge tube, and 1 mL of pre-cooled methanol-acetonitrile-water (2:2:1, *v/v*) solution was mixed with the sample. The mixture was vortexed, ultrasonically extracted for 30 min, stood in −20 °C for 10 min, and then centrifuged at 14,000 g for 20 min. After the supernatant was vacuum-dried, it was reconstituted with 100 μL of water-acetonitrile (1:1, *v/v*), vortexed for 1 min, and centrifuged at 14,000 g for 15 min, and the supernatant was used for analysis. A quality control (QC) sample was prepared by mixing aliquots of all the individual treated samples (10 μL).

2.3. Data analysis

For drug metabolism analysis, the following software was used: Xcalibur™ 3.1, Compound Discoverer 3.1 and Mass Frontier 7.0 (Thermo Fisher Scientific, Waltham, MA, USA). The raw data were acquired and processed using Xcalibur™ 3.1, which was used for qualitative and quantitative analysis of CPZ and its metabolites. The Compound Discoverer software was used for screening of metabolites of CPZ through the workflow of detection of expected metabolites of CPZ and non-targeted compounds. The workflow mainly included spectra alignment, compound detection, grouping, compound prediction, and database retrieval from mzCloud and ChemSpider, which was referred to our previous work [26]. Thermo Xcalibur Qual Browser and Mass Frontier 7.0 were used to predict the elemental composition of fragment ions and assist mass spectrometry fragmentation analysis.

For metabolomic analysis of fish endogenous substances, the raw data were converted to mzXML files using ProteoWizard MSConvert before importing into freely available XCMS software. XCMS software was used for peak detection, extraction, alignment, and integration from the raw data. Compound identification was performed by setting accurate mass error below 25 ppm, and MS/MS spectra were interpreted with an in-house database (Shanghai Applied Protein Technology) established with available authentic standards. Statistical data analysis was performed using R package models for *t*-test, principal component analysis (PCA) and orthogonal partial least squares discriminant analysis (OPLS-DA). A variable importance in projection (VIP) score of OPLS-DA model and *t*-test were applied to rank the metabolites best distinguished between treated and control groups. The screening criteria for significantly differential metabolites were VIP $>$ 1 and p value $<$ 0.05. In cluster analysis, the response signal intensity of the differential metabolites was normalized by subtracting the average signal intensity of all samples and then dividing by the root mean square. The pathway analysis in MetaboAnalyst 5.0 (https://www.metaboanalyst.ca/MetaboAnalyst/) was used to elucidate which metabolic pathways in fish were affected by CPZ exposure. The metabolic pathways with p values $<$ 0.05 were selected as the main pathways through which CPZ affects the metabolism of endogenous substances in fish.

2.4. Toxicity prediction software

The *in-silico* prediction of drug toxicity was carried out by following free available tools: Ecological Structure-Activity Relationship (ECOSAR v1.11) to estimate ecotoxicity and Toxicity Estimation Software Tool (TEST) (v5.1.2) to predict ecotoxicity and developmental toxicities.

3. Results and discussion

3.1. Targeted and non-targeted metabolic analysis strategies of CPZ in grass carp

In this study, CPZ metabolites were systematically screened and identified in different tissues of grass carp using UHPLC-Q-Orbitrap MS, and accurate quantitative and semi-quantitative analyzes of CPZ and its metabolites were performed. We used serum, liver and muscle tissues of grass carp as research objects. The serum can provide a system-wide perspective on the presence of drug, the liver reveals the metabolic process of the drug, and the muscle, as an edible part, is the main object of food safety testing. The analytical strategy consisted of three main steps: (1) Serum, liver and muscle tissues were respectively collected from the treatment and control groups, and CPZ and its metabolites were extracted using corresponding sample preparation methods for subsequent analysis. (2) Data-acquisition was performed in full scan mode at a resolution of 70,000. The $ddMS^2$ mode was employed to obtain secondary mass spectrometry (MS^2) data. In $ddMS^2$ mode, the precursor ions of the top 10 signals were selected and further fragmented into related fragment ions. (3) The raw data acquired was imported into Compound Discoverer and Qual Browser software to identify unknown metabolites and make predictions of expected compounds. In summary, the molecular structures of metabolites were elucidated based on the accurate mass, fragment ions, fragmentation patterns, mzCloud and ChemSpider databases, and literature reports. The isomers could not be accurately identified due to the same molecular formula and similar MS/MS spectra. Therefore, the octanol-water partition coefficients (Log K_{ow}) corresponding to different structural formulas were estimated by EPISuite KOWWIN v1.69 to provide a reference for the identification of isomers. Compound with higher Log K_{ow} value generally indicates stronger hydrophobicity and longer retention time (t_R) in reversed-phase liquid chromatography [27,28].

3.2. Metabolite identification of CPZ

In order to obtain a global view of the metabolite profile of CPZ in grass carp, the metabolites in serum, liver and muscle tissues were examined. The identification of CPZ metabolites was performed based on the above strategy. A total of 13 metabolites of CPZ was detected using the non-targeted screening strategy, of which 5 metabolites were confirmed by the targeted strategy using authentic standards. The extracted ion chromatograms of CPZ and its metabolites in liver tissue are exhibited in Fig. 1, and those in serum and muscle tissues in Fig. S1. The metabolites were generated mainly from the reactions such as oxygenation, demethylation, dechlorination and carboxylation reactions, and 6, 13, and 13 compounds were detected in serum, liver and muscle samples, respectively. As a result, all 13 metabolites were identified, including 11 previously reported and 2 newly identified metabolites (M9 and M13), and 5 of the previously reported metabolites (CPZSO M1, 7-HOCPZ M2, NOCPZ M3, DMCPZ M7 and PZ M10) were confirmed using respective authentic standards. The detailed information of the metabolites is listed in Table 1. The mass spectra and the deduced molecular structure corresponding to fragment ions of CPZ metabolites are shown in Fig. S2, and MS^2 information of fragmentation

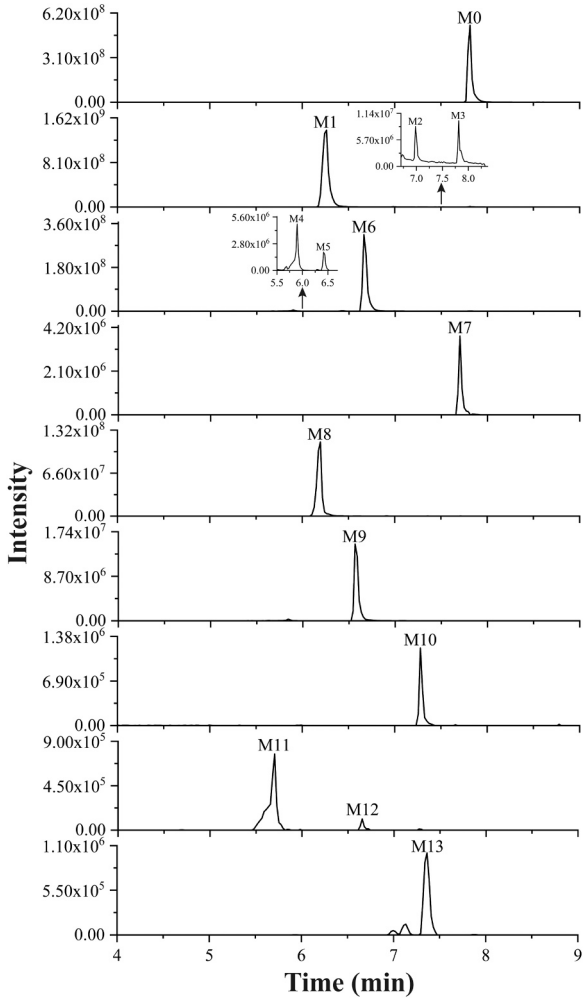

Fig. 1. The extracted ion chromatograms of CPZ and its metabolites in liver tissue on the 1st day after withdrawal of treatment.

ions is shown in Table S1. The following was a putative identification analysis and structural derivation of metabolites.

3.2.1. Fragmentation pathway of CPZ

The molecular structure and MS^2 fragmentation mechanism of the metabolites is similar to that of the parent drug [29]. To facilitate the elucidation of the molecular structure of CPZ metabolites, the fragmentation pattern of CPZ was investigated. The parent drug (M0) was eluted in liquid chromatography at 7.79 min and its quasi-molecular ion $[M + H]^+$ by following mass spectrometry was *m/z* 319.1030 ($C_{17}H_{19}ClN_2S$) with a mass error of −1.9 ppm. The fragmentation pathway of CPZ has been speculated in our previous work [26], as shown in Fig. S3. By observing the MS^2 spectral data of CPZ combined with Qual Browser and Mass Frontier software, it was found that the parent successively lost N,N-dimethylpropylamine chain at the N position of the phenothiazine, and then underwent dechlorination and desulfuration, producing a series of characteristic fragment ions at *m/z* 274.0452, 246.0139, 239.0763, 233.0060, 214.0418, 86.0964 and 58.0651. Among them, *m/z* 246.0139, 86.0964 and 58.0651 fragment ions had higher abundance and were the required diagnostic fragment ions. They are also qualitative and quantitative ions used in the official standard methods using high-performance liquid chromatography tandem triple quadrupole mass spectrometry [30,31].

3.2.2. Multiple metabolites based on oxygenation reactions

Oxygenation is the common metabolic pathway for CPZ, mainly including the sulfoxide of sulfur, oxidation of nitrogen in tertiary amine group and hydroxylation of benzene ring. Metabolites M1, M2 and M3 presented $[M + H]^+$ ion at *m/z* 335.0979 with mass errors of −2.7, −2.1 and −3.0 ppm, respectively. The molecular formula of M1, M2 and M3 was identified as $C_{17}H_{19}ClN_2OS$, which was an oxygen atom (O, 16 Da) more than that of CPZ. They as isomers were respectively eluted at 6.22, 6.98 and 7.81 min, and were identified by authentic standards as known targeted metabolites, corresponding to CPZSO (M1), 7-HOCPZ (M2) and NOCPZ (M3), respectively.

Metabolites M4, M5 and M6 presented $[M + H]^+$ ion at *m/z* 351.0929 with mass errors of −2.6, −3.4 and −2.8 ppm, respectively. Their accurate mass was 32 Da (O_2) more than that of CPZ, which had diagnostic fragment ions of CPZ such as *m/z* 86.0964 and 58.0651, and the molecular formula was identified as $C_{17}H_{19}ClN_2O_2S$. They as isomers were respectively eluted at 5.90, 6.41 and 6.66 min. M5 showed the distinctive fragment ion of *m/z* 102.0913 ($C_5H_{12}NO^+$), which resulted from the oxidation of the nitrogen atom. Moreover, M5 also had fragment ions similar to CPZ and CPZSO, such as *m/z* 290.0401, 273.0373, 255.0712, 233.0060, 231.9982. Therefore, M5 was putatively identified as the oxidation product with the reaction site at the sulfur atom or benzene ring and tertiary amine. Metabolites M4 and M6 had fragment ions of *m/z* 306.0350 ($C_{15}H_{13}ClNO_2S^+$) and *m/z* 278.0037 ($C_{13}H_9ClNO_2S^+$), respectively, indicating that the oxygenation reaction occurred on the phenothiazine structure, generating sulfoxide and

Table 1
The detailed information for CPZ and its metabolites.

Compound	Observed (*m/z*)	Theoretical (*m/z*)	Error (ppm)	t_R (min)	Formula	Composition Change	Transformations	Log K_{ow}	Reported (Reference)
CPZ (M0)	319.1024	319.1030	−1.9	7.79	$C_{17}H_{19}ClN_2S$	/	/	5.21	[20]
CPZSO (M1)	335.097	335.0979	−2.7	6.22	$C_{17}H_{19}ClN_2OS$	+ (O)	Oxygenation	2.98	[20]
7-HOCPZ (M2)	335.0972	335.0979	−2.1	6.98	$C_{17}H_{19}ClN_2OS$	+ (O)	Oxygenation	4.37	[22]
NOCPZ (M3)	335.0969	335.0979	−3.0	7.81	$C_{17}H_{19}ClN_2OS$	+ (O)	Oxygenation	4.44	[20]
M4	351.092	351.0929	−2.6	5.90	$C_{17}H_{19}ClN_2O_2S$	+ (O_2)	Oxygenation, Oxygenation	2.15	[33]
M5	351.0917	351.0929	−3.4	6.41	$C_{17}H_{19}ClN_2O_2S$	+ (O_2)	Oxygenation, Oxygenation	2.21	[20]
M6	351.0919	351.0929	−2.8	6.66	$C_{17}H_{19}ClN_2O_2S$	+ (O_2)	Oxygenation, Oxygenation	3.54	[33]
DMCPZ (M7)	305.0867	305.0874	−2.3	7.68	$C_{16}H_{17}ClN_2S$	− (CH_2)	Demethylation	4.99	[22]
M8	321.0817	321.0823	−1.9	6.18	$C_{16}H_{17}ClN_2OS$	− (CH_2) + (O)	Demethylation, Oxygenation	2.77	[35]
M9	337.0763	337.0772	−2.7	6.56	$C_{16}H_{17}ClN_2O_2S$	− (CH_2) + (O_2)	Demethylation, Oxygenation, Oxygenation	1.94	Our work
PZ (M10)	285.1414	285.1420	−2.1	7.27	$C_{17}H_{20}N_2S$	− (Cl) + (H)	Reductive Dechlorination	4.56	[20]
M11	301.1361	301.1369	−2.7	5.69	$C_{17}H_{20}N_2OS$	− (Cl) + (HO)	Oxygenation, Reductive Dechlorination	2.34	[20]
M12	301.1365	301.1369	−1.3	6.64	$C_{17}H_{20}N_2OS$	− (Cl) + (HO)	Oxygenation, Reductive Dechlorination	3.73	[21]
M13	349.0763	349.0772	−2.6	7.37	$C_{17}H_{17}ClN_2O_2S$	− (H_2) + (O_2)	Demethylation, Carboxylation	3.97	Our work

hydroxyl functional groups. In combination of the structural information of the fragment ions and the chromatographic retention behavior judgment based on the Log K_{ow} of the metabolites of different structural formulas, M4, M5 and M6 were tentatively identified as shown in Fig. 2, and the corresponding Log K_{ow} values were 2.15, 2.21 and 3.54, respectively. Their mass spectra and the deduced molecular structure corresponding to fragment ions are shown in Fig. S2.

It was reported that degradation products (*m/z* 351.0929) were observed when exploring the photocatalytic and photolytic conversion of CPZ under aerobic conditions, but only the degradation pathway was discussed and its molecular structure was not analyzed [32]. Degradation of CPZ via Fenton process has been reported, and the deduced products were generated only from hydroxylation of the parent drug [33]. In our previous degradation study of CPZ under different conditions, only one degradation product M5 was found [26]. Here, the double oxide identification of CPZ was further improved and supplemented through *in vivo* metabolism study of CPZ in grass carp.

3.2.3. Multiple metabolites based on demethylation reactions

Metabolite M7 presented $[M+H]^+$ ion at *m/z* 305.0874 ($C_{16}H_{17}ClN_2S$) with mass error of −2.3 ppm. M7 was 14 Da (CH_2) less than that of CPZ, and was eluted at 7.68 min, which had a diagnostic fragment ion of *m/z* 72.0808 ($C_4H_{10}N^+$) for N-demethylation and multiple fragment ions identical to CPZ such as *m/z* 274.0452, 246.0139, 239.0763 and 214.0418. M7 was produced by N-demethylation of CPZ, which was also an oxidation pathway, and it was known targeted metabolite identified by authentic standard, corresponding to DMCPZ.

Metabolite M8 presented $[M+H]^+$ ion at *m/z* 321.0823 with mass error of −1.9 ppm and was eluted at 6.18 min. The molecular formula was predicted to be $C_{16}H_{17}ClN_2OS$. Compared with M7, the change in element composition was the addition of one O, and it was speculated that M8 was produced by demethylation and oxygenation reactions. Based on the MS^2 information, the deduced MS fragmentation mechanism of M8 is shown in Fig. S2. M8 had a diagnostic fragment ion of *m/z* 72.0808 ($C_4H_{10}N^+$) for N-demethylation and multiple fragment ions identical to CPZ and the metabolite CPZSO as shown in Table S1. Since the parent CPZ is more likely to produce a functional group with a sulfoxide structure [34], the deduced structural formula of M8 was mainly from CPZ through sulfoxide of sulfur and N-demethylation. M8 was one of the metabolites of CPZ in rat [35].

Metabolite M9 presented $[M+H]^+$ ion at *m/z* 337.0772 with mass error of −2.7 ppm and was eluted at 6.56 min. The molecular formula was predicted to be $C_{16}H_{17}ClN_2O_2S$. Compared with M8, the change in element composition was the addition of one O. From the mass spectrum of M9, it could be observed that there was a diagnostic fragment ion of *m/z* 72.0808 ($C_4H_{10}N^+$) with high abundance of N-demethylation. In addition, the fragment ions of *m/z* 86.0968 and 58.0658 with lower abundance were observed, which mainly corresponded to the structure of tertiary amine, but contradicted with the actual structure of secondary amine. Since the accurate masses of M9 and the isotopic peak (*m/z* 337.0950) of CPZSO (*m/z* 335.0979) were close, and the baseline of CPZSO was higher in the chromatogram (Fig. 1) implying there were CPZSO residues at the same t_R, it was speculated that *m/z* 86.0968 and 58.0658 might be the mass spectrum interference caused by the fragment ions of the CPZSO isotope peak. Based on the MS^2 information, the deduced molecular structure corresponding to the fragment ions of M9 is shown in Fig. S2. Due to the presence of fragment ion of *m/z* 278.0037 ($C_{13}H_9ClNO_2S^+$), it indicated that the oxygenation site located on the phenothiazine structure, so the molecular structure was speculated to be as shown in Fig. 2. CPZ mainly underwent hydroxylation of benzene rings, sulfoxide of sulfur, and N-demethylation to convert to M9, which was one new CPZ metabolite identified for the first time.

3.2.4. Multiple metabolites based on dechlorination reactions

Metabolite M10 presented $[M+H]^+$ ion at *m/z* 285.1420 with mass error of −2.1 ppm and was eluted at 7.27 min. The molecular formula

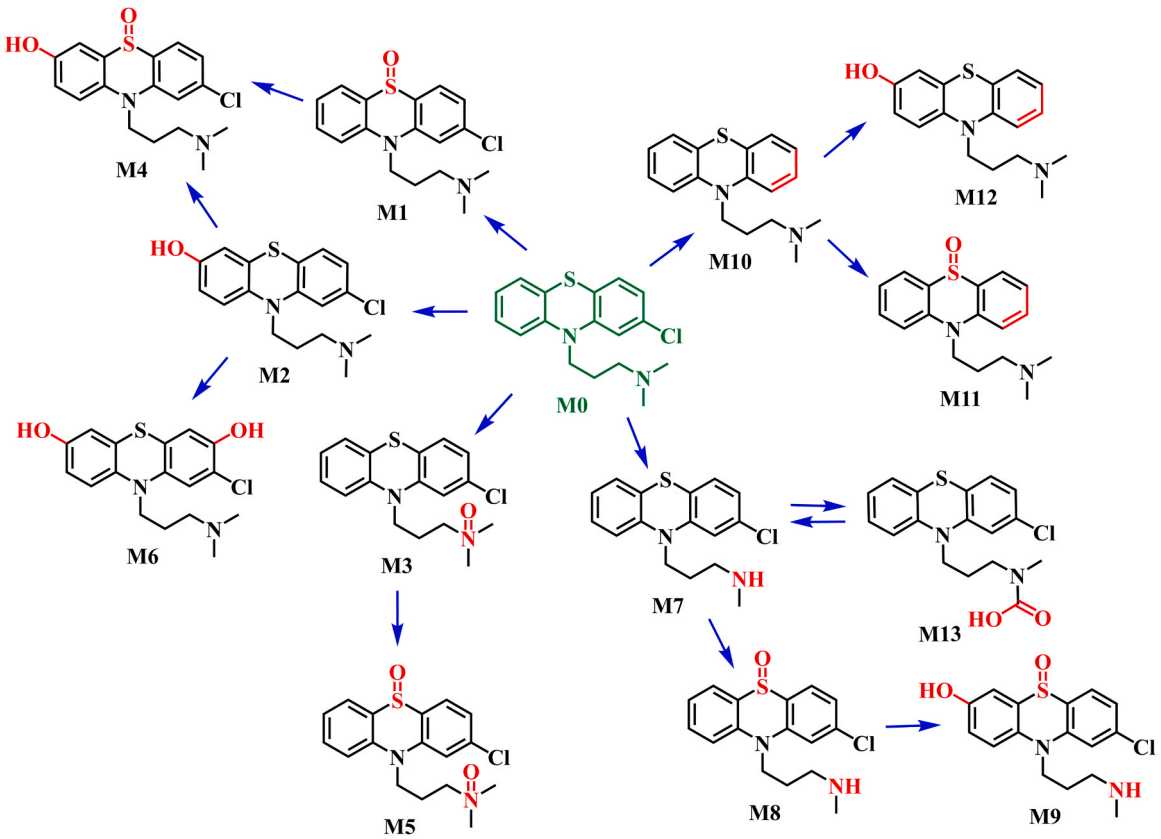

Fig. 2. The transformation pathways and possible structures of CPZ and its metabolites.

was predicted to be $C_{17}H_{20}N_2S$. Compared with CPZ, the change in element composition was the subtraction of one chlorine (Cl) and the addition of one hydrogen (H). M10 had diagnostic fragment ions of CPZ such as *m/z* 86.0964 and 58.0651, which was identified by authentic standard as known targeted metabolite, corresponding to PZ.

Metabolites M11 and M12 presented $[M + H]^+$ ion at *m/z* 301.1369 with mass errors of −2.7 and −1.3 ppm, respectively. Their accurate mass was 16 Da (O) more than that of PZ (M10), which had diagnostic fragment ions of CPZ such as *m/z* 86.0964 and 58.0651. Therefore, the molecular formula was identified as $C_{17}H_{20}N_2OS$. They as isomers were respectively eluted at 5.69 and 6.64 min. M11 had fragment ions similar to PZ, such as *m/z* 199.0449 ($C_{12}H_9NS^{\bullet+}$) and 212.0517 ($C_{13}H_{10}NS^+$). However, the position of the oxygenation could not be verified based only on its MS^2 data. Metabolite M12 had fragment ion of *m/z* 196.0767 ($C_{13}H_{10}NO^+$), indicating that the oxygenation occurred on the phenothiazine structure, generating hydroxyl functional group. According to the chromatographic retention behavior judgment based on the Log K_{ow} of different structural formulas, M11 and M12 were tentatively identified, and their deduced molecular structures are shown in Fig. 2, and the Log K_{ow} values of M11 and M12 were 2.34 and 3.30, respectively. Dechlorination reactions of CPZ have been reported also during Fenton process [33] and photodegradation process [20,21].

3.2.5. The metabolite based on carboxylation reaction

Metabolite M13 presented $[M + H]^+$ ion at *m/z* 349.0772 with mass error of −2.6 ppm and was eluted at 7.37 min. The molecular formula was predicted to be $C_{17}H_{17}ClN_2O_2S$. Compared with the parent CPZ, the change in element composition was the subtraction of two hydrogen atoms (H_2) and the addition of two oxygen atoms (O_2). The molecular structure of M13 screened out from the mzCloud database by the Compound Discoverer software is shown in the Fig. 2. M13 had a diagnostic fragment ion of *m/z* 72.0808 ($C_4H_{10}N^+$) and multiple fragment ions identical to other metabolites such as *m/z* 321.0823, 273.0373, 233.0060, 231.9982. Studies have reported that amino compounds may be susceptible to carboxylation by dissolved carbon dioxide, converting them to the corresponding carbamic acid derivatives, such as the secondary amine structure of the antidepressant drug sertraline that is metabolized to the carbamate acid [36]. Therefore, M13 was presumed to be produced by a carboxylation reaction of M7 after demethylation of CPZ, which was another newly identified metabolite, and the reaction process was reversible [37].

Since the toxicity of many CPZ metabolites is currently unknown, their residues in fish pose risks to consumer safety. Through the research of the metabolism of CPZ in grass carp, this work achieved the identification of CPZ and its metabolites in complex matrices, which could provide an important reference for the study of the metabolic mechanism of CPZ.

3.3. Quantitative analysis of targeted analytes

This study explored the changes in the content levels of CPZ and its metabolites in different fish tissues (serum, liver and muscle) over time through quantitative analysis of CPZ and its metabolites in samples collected at different breeding times, including verification of the quantitative ability of CPZ and its metabolites in different samples, accurate quantitative analysis of CPZ and its four targeted metabolites, and semi-quantitative analysis of other identified CPZ metabolites.

The MS^2 spectra of different samples were compared with those of standard solutions of CPZ and its four metabolites (CPZSO, 7-HOCPZ, DMCPZ and PZ). The results showed that the MS^2 spectra of targeted analytes in the samples were in good agreement with those of their standard solutions. The isotope internal standard method was used to compensate for matrix effects and losses caused by sample preparation [38,39]. The calibration curves were established using eight concentration levels ranging from 0.2 to 200 μg L^{-1} (0.2, 0.5, 1, 5, 10, 50, 100 and 200 μg L^{-1}) with the isotopic internal standard solution CPZ-D6 at 5 μg L^{-1} for quantitative analysis of these five compounds in serum, liver and muscle tissues at the different time of keeping in clean water after exposure to CPZ. As shown in Table S2, the linearity was achieved for all targeted analytes with the correlation coefficients (R^2) above 0.9998. The recovery was validated for the targeted analytes in serum, liver and muscle samples as shown in Fig. S4. The spiking recoveries of the five compounds were in the range of 72.5 %-110.7 %. Reproducibility was evaluated in triplicate by measuring the relative standard deviations (RSDs) of recoveries for spiked serum, liver and muscle samples, respectively, and RSDs were in the range of 2.5 %-11.3 %, which met the analysis requirements for trace drug residues in foodstuff.

The previous study had shown that CPZ is relatively stable in the absence of light but can be degraded under light conditions [20], among which CPZSO is both a metabolite and a photolysis product of CPZ. In order to be more in line with the actual situation, the actual lighting of a day was used. After the application of CPZ, the initial water samples were tested. At this time, the concentration of CPZ in water was 407.7 ± 11.3 μg L^{-1}, and the water contained a small amount of CPZSO with a concentration of 5.5 ± 0.1 μg L^{-1}. Water samples collected one day after the application of CPZ were tested and the concentration of CPZ was 0.6 ± 0.01 μg L^{-1}, while the concentration of CPZSO was 157.7 ± 3.7 μg L^{-1}. The degradation of CPZ in water was a continuous process, and fish were constantly exposed to the drug in this raising water. The quantitative analysis in this study mainly focused on the actual change trends of drug residues in different fish tissues, and the change trends of content levels of CPZ and its four metabolites in different tissues are presented in Fig. 3. The standard deviation of multiple measurements was used to express standard uncertainty (u) of the result [40,41].

The metabolism behaviors of the parent drug CPZ and its metabolites were similar in the different tissues with a high content on the 1st day after withdrawal of CPZ treatment, followed by a gradual decrease in concentrations over time. The bioconcentration factor (BCF) of a drug was estimated by dividing the content level in fish by that in the raising water [42]. The content level of CPZ in the raising water was a dynamically changing state. Here, it is assumed that the content level of CPZ in the raising water is 0.5 mg L^{-1}. The results showed that CPZ was accumulated significantly in the liver and muscle on the 1st day after withdrawal of treatment. The content levels of CPZ in the liver and muscle were 4.3 and 3.7 times that in the raising water respectively, while the concentration of CPZ in serum was relatively low with the BCF of 0.2. In addition, it could be inferred from the content levels of metabolites that a high proportion of the parent drug had undergone metabolic or degradative transformation. Among them, CPZSO was the most abundant metabolite in all the tissues, and its contents in serum, liver and muscle tissues were 4–14 times that of CPZ in corresponding tissues on the 1st day after withdrawal of treatment. On the 7th day after withdrawal of treatment, the parent drug was no longer detectable in the serum, while CPZSO still had a concentration of 53.2 ± 9.6 μg kg^{-1}. The contents of CPZSO in liver and muscle samples at this time were 8 and 56 times that of the parent drug, respectively. It has been shown in the literature that CPZSO is one of the main metabolites of CPZ [34,35], and moreover, the content of CPZSO is the highest among its degradation products in our previous degradation study [26]. Therefore, it was concluded that CPZSO is an important characteristic metabolite of CPZ. In addition, for other targeted metabolites, 7-HOCPZ, DMCPZ and PZ were not detected in all serum samples. With the progress of metabolism, however, except for a small amount of 7-HOCPZ, DMCPZ and PZ in liver and muscle samples could not be detected on the 7th day after withdrawal of treatment.

At the same time, for other metabolites identified by non-targeted metabolism, semi-quantitative analysis was performed using the calibration curve of CPZ as a reference. The content levels in serum, liver and muscle samples are shown in Tables S3-S5. From the results, it could be found that most metabolites were further converted quickly or excreted from the body over time. The metabolites M6, M8 and M9 (the hydroxylation, sulfoxide and N-demethylation products of CPZ) should

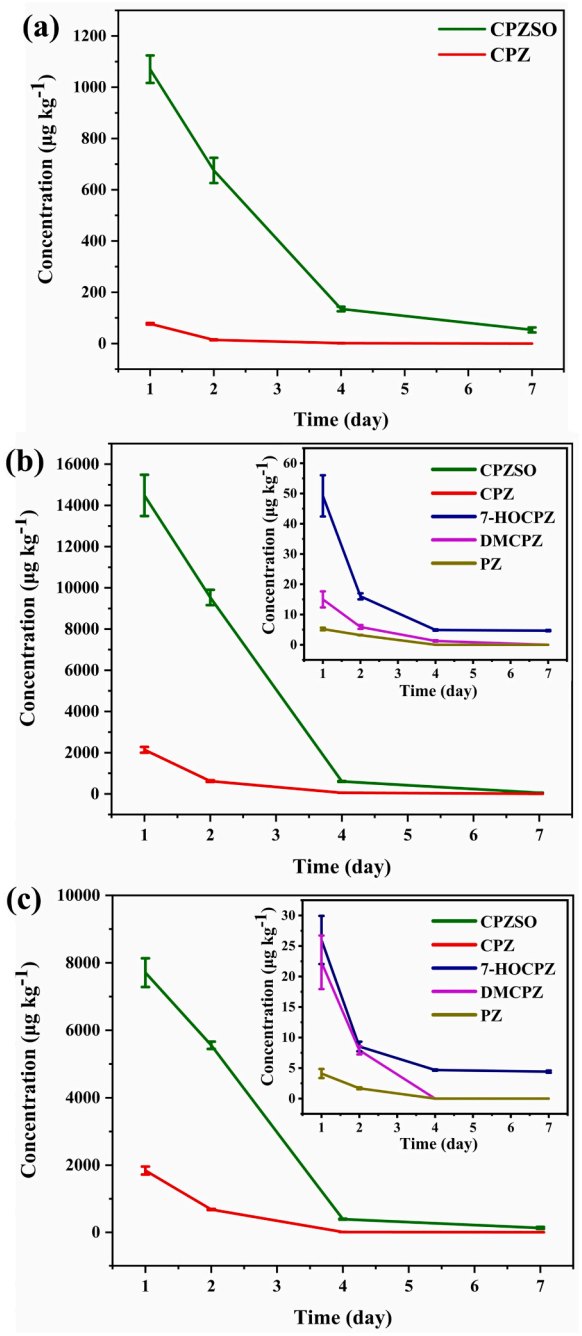

Fig. 3. The content trends of targeted analytes in different tissues. a: serum, b: liver, c: muscle.

be noticed, which were present at relatively high content levels and could still be detected on the 7th day after withdrawal of treatment. Among them, the concentrations of M6 in liver and muscle samples were 91.2 ± 6.9 and 37.3 ± 4.4 μg kg^{-1}, respectively, even higher than those of the parent drug on the 7th day after withdrawal of treatment. Therefore, in addition to characteristic metabolite CPZSO, other metabolites with high content should also be paid attention to.

The liver is the main target organ for drug metabolism [43]. From the quantitative results, it could be seen that the metabolites contents of grass carp were highest in the liver tissues, but the contents were also relatively high in the muscle tissues. Therefore, CPZ metabolites in edible parts of fish might be a potential risk.

3.4. In-silico toxicity prediction

The toxicity of most CPZ metabolites is unknown and the experimental toxicological data of the metabolites are currently unavailable. In order to gain a preliminary understanding of their harmfulness, the toxicity of CPZ and its metabolites was estimated through two toxicity prediction software using different models [44]. ECOSAR is mainly based on factors such as structural similarity, toxic groups, and physicochemical properties to predict the toxicity of compounds [45]. ECOSAR was used to predict the toxicity of CPZ and its metabolites, primarily based on log K_{ow} and chemical structure with predictions obtained by classifying them as aliphatic amines. TEST predicts the toxicity of compounds by using quantitative structure activity relationships (QSARs) methodologies that are mathematical models used to predict toxicity measurements based on physical characteristics of the molecular structure of compounds [46]. In TEST, the consensus method for the prediction of ecotoxicity and developmental toxicities was adopted. Tables S6 and S7 present the predicted toxicity results of CPZ and its metabolites for different species by ECOSAR and TEST, respectively.

The log K_{ow} value of CPZ was greater than those of the metabolites as listed in Table 1. The ECOSAR results showed that the overall toxicity of the metabolites was less than that of CPZ, while individual prediction values were close to CPZ, such as 7-HOCPZ, NOCPZ, DMCPZ and PZ. This toxicity is also consistent with the trends for drugs to be more easily converted into more polar and relatively lower toxic metabolites *in vivo* [47]. The previous study reported using the following toxicity levels to judge the acute and chronic toxicity of a substance for fish and *Green algae*: high-toxicity ($x < 1$ mg/L), moderate-toxicity ($1 < x < 10$ mg/L), low-toxicity ($10 < x < 100$ mg/L) and no-harmful ($x > 100$ mg/L) [48]. For fish, CPZ and DMCPZ were of high-toxicity. The metabolites from sulfoxide of sulfur such as CPZSO, M4, M5, M8, M9 and M11 were of low-toxicity, while the remaining metabolites were of moderate-toxicity. For *Green algae*, the toxicity levels of the metabolites were of high-toxicity or moderate-toxicity.

The TEST results showed that the toxicity of the metabolites of CPZ at the two species of *Daphnia magna* and *Tetrahymena pyriformis* was generally lower than that of CPZ, or the toxicity was similar. However, the toxicity results of the *Fathead minnow* showed that many of the metabolites were higher toxic than CPZ, such as CPZSO, NOCPZ, M5, M6 and M13, especially NOCPZ and M6, which were 2.9 times and 1.9 times higher toxic than CPZ. For the predicted developmental toxicity, both CPZ and the metabolites had developmental toxicity. There has been report of using TEST to predict the toxicity of CPZ and its degradation products [20]. Since the version of TEST underwent continuous update and optimization, its functions and prediction accuracy have been greatly improving [49]. On the basis of chemical structure, the prediction results by QSARs method may differ numerically, but also indicate that the toxicity of some transformation products is similar to or higher than that of CPZ.

A study investigated the ecotoxicological effects of CPZ on freshwater goldfish (*Carassius auratus*) using the toxic culture experiment, and the median lethal concentration (LC_{50}) of CPZ for goldfish in 24, 48 and 96 h was 1.11, 0.43 and 0.32 mg L^{-1}, respectively, which was likely to cause liver damage [50]. The results showed that the experimental results were consistent with the predicted results of this study regarding the toxicity of CPZ exposure to fish. Studies have found that CPZ and its metabolites are photomutagenic under light conditions, and the demethylation products can cause extensive DNA photodamage that is difficult to repair by cells [24]. In existing toxicological studies, there are a few toxicological data for CPZ and its metabolites. For example, the median lethal dose (LD_{50}) of CPZ, CPZSO and 7-HOCPZ for mouse or rat via intraperitoneal administration was 58, 163 and 119 mg kg^{-1}, respectively. PZ itself can be used as a phenothiazine drug, similar to CPZ, and will affect endocrine function, increase sensitivity to sunlight, and cause hemolytic anemia (sourced from PubChem, https://pubchem.

ncbi.nlm.nih.gov/). Although toxicological data for some metabolites are lacking, CPZ belongs to the phenothiazine class of drugs, and its metabolites retain the basic structure of phenothiazine, and most of these metabolites exhibit similar activity, suggesting that the toxicological mechanisms may be similar [51]. The *in-silico* predicted ecotoxicity and developmental toxicities also confirmed the adverse toxic effects of the previously reported metabolites to a certain extent. Nevertheless, it must be pointed out that the toxicity of more metabolites has not yet been evaluated and verified by experimental outcome. The toxicity predicted is only for reference, and subsequent research is still needed to supplement the actual toxic data.

3.5. Effect of CPZ exposure on the metabolome of grass carp

Metabolomics is a promising tool for assessing the health of aquatic organisms [52]. Muscle is a metabolically active tissue that plays an important role in energy balance and metabolism. In this study, non-targeted metabolomic analysis of endogenous substances in grass carp was conducted using muscle as the exemplary tissue to explore the effect of CPZ exposure on the metabolome of grass carp. Data from both positive and negative ion modes were collected to improve the metabolite coverage. PCA score plots of the QC sample and all experimental samples were used to observe the overall distribution of samples, as well as the stability of the entire analytical process, as shown in Fig. S5. The tightly clustered QC samples indicated the stability of detection and the high reproducibility of the acquired data. Compound identification was performed by an in-house database established with available authentic standards. A total of 1125 metabolites were identified, including 502 metabolites in the positive ion mode and 623 metabolites in the negative ion mode. Based on the classification information of metabolites, a statistical map of annotated endogenous metabolites was drawn, as shown in Fig. S6.

Statistical data analysis with *t*-test, PCA, and OPLS-DA was performed for the treatment and control groups. PCA was used as an unsupervised approach to visualize the segregation of metabolites between the two groups. As shown in Fig. 4, the model parameters of PCA were as follows: $R^2X = 0.541$ in positive ion mode and 0.637 in negative ion mode, where R^2X represents the model explanation rate. The PCA score plots showed that the metabolic profiles were clearly separated, indicating the different metabolic profiles between groups. OPLS-DA was used as a supervised approach to visualize the segregation of metabolites between the two groups, as shown in Fig. 4. The model parameters of OPLS-DA were as follows: $R^2Y = 0.995$ in positive ion mode and 0.996 in negative ion mode; $Q^2 = 0.575$ in positive ion mode and 0.516 in negative ion mode, where R^2Y and Q^2 represent the robustness of the model. The results of OPLS-DA showed that R^2Y was close to 1 between treatment and control groups, and $Q^2 > 0.5$, suggesting that the model can be used to screen metabolites. The OPLS-DA model was used for 200 response sequencing tests, showing that the prediction effect of this model is good without over-fitting. Screening for significant differential

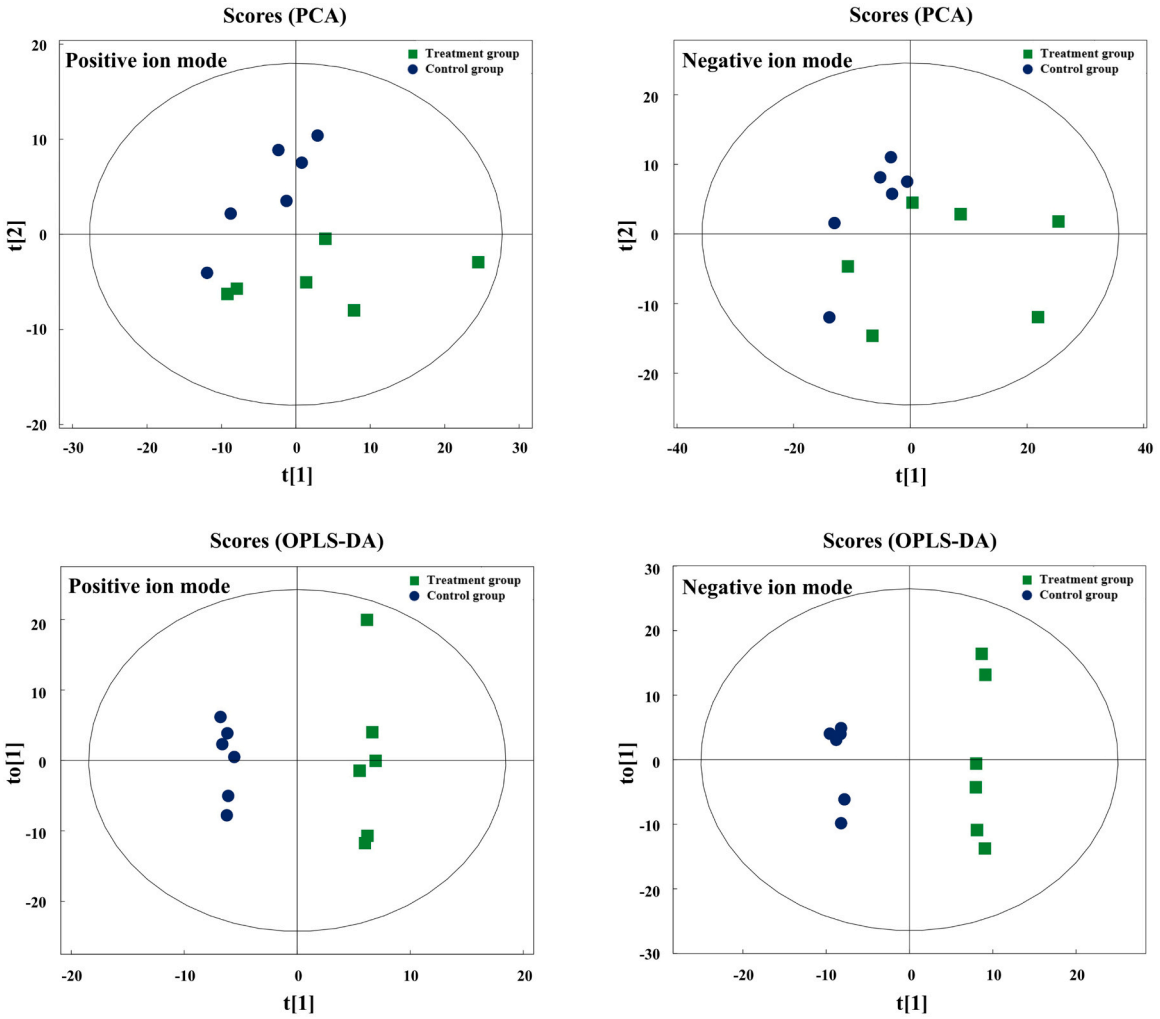

Fig. 4. PCA and OPLS-DA score plots based on CPZ treatment and the control groups in positive and negative ion modes. t[1], t[2], to[1] represent different principal components respectively.

metabolites was performed using VIP value (VIP > 1) of OPLS-DA and *p* value ($p < 0.05$) of *t*-test. In the positive and negative ion modes, 26 and 23 significant differential metabolites were screened respectively, as shown in Tables S8 and S9. Cluster analysis was performed on the significantly differential metabolites, and the heat maps in positive and negative ion modes are shown in Fig. S7.

We found by direct observation that fish exhibited anxiety-like behavior including high speed and abnormal swimming after exposure to CPZ at administration dosage. To explore the potential metabolic pathways disordered by CPZ exposure on fish, significant differential metabolites were subjected to metabolic pathway enrichment analysis using the KEGG database. As shown in Fig. S8 and Table S10, nine significantly differential metabolic pathways ($p < 0.05$) were found, including the Pantothenate and CoA biosynthesis, Arginine biosynthesis, Histidine metabolism, Nitrogen metabolism, Pyruvate metabolism, Alanine, aspartate and glutamate metabolism, Phenylalanine metabolism, Glyoxylate and dicarboxylate metabolism, and Phenylalanine, tyrosine and tryptophan biosynthesis. Five out of nine metabolic pathways showed alterations in amino acid metabolism. Some matched metabolites in the metabolic pathways have been found. Aspartic acid, glutamic acid and glutamine showed an up-regulation trend, which was related to multiple significantly differential metabolic pathways, such as Alanine, aspartate and glutamate metabolism, Arginine biosynthesis and Nitrogen metabolism. The studies with mammals and fish indicated that glutamate, aspartate, and glutamine are the important energy substrates for their small intestine [53]. Glutamate and aspartate are excitatory neurotransmitters, and their upregulation would associate with the excitatory behavior of the fish [54]. Valine is a branched chain amino acid that accounts for one-third of the branched amino acids absorbed in muscles and is responsible for strengthening and replenishing muscle tissue. The significant upregulation of valine levels detected in this study might be related to abnormal movement of fish [55]. The study has shown that sedative drug can cause zebrafish eleuthero-embryos to become hyperactive [56]. The KEGG pathway was indicative of metabolic disorder in the endogenous metabolome of grass carp, which was a toxic mechanism.

4. Conclusions

This work mainly elucidated the drug metabolic mechanism of CPZ in fish based on reliable targeted and non-targeted screening methods using high resolution mass spectrometry. Thirteen CPZ metabolites were identified, including 11 previously reported and 2 newly identified metabolites (M9 and M13), and 5 of the previously reported metabolites were confirmed using authentic standards. The findings revealed that the metabolism of CPZ mainly involved oxygenation, demethylation, dechlorination, and carboxylation reactions, among which oxygenation was the main metabolic pathway. Accurate quantitative analysis of CPZ and its known targeted metabolites indicated that the concentrations of CPZSO in different tissues were higher than that of CPZ, and it was an important representative metabolite of CPZ. Toxicity prediction results showed that the ecotoxicity of some metabolites was similar to or even higher than that of CPZ, and they all had developmental toxicity. Metabolomic analysis showed that CPZ exposure could cause metabolic disorder in the endogenous metabolome of grass carp. This study made up for the lack of research on the metabolic transformation of CPZ in aquatic animals and provided a reference for the risk assessment of CPZ in the aquaculture as well as environment.

Environmental implication

CPZ residues are frequently detected in aquatic animals and in environmental waters, transforming into various unknown toxic products due to environmental and biological factors. These residues can bioaccumulate through the food chain, posing risks to humans. However, there have been no reports on the *in-vivo* metabolism of CPZ in aquatic species so far. This study made up for the lack of research on the metabolic transformation of CPZ in aquatic animals and provided a reference for the risk assessment of CPZ in the aquaculture as well as environment.

CRediT authorship contribution statement

Sen Zhang: Visualization, Software, Methodology, Investigation. **Jinxia Dai:** Writing – original draft, Visualization, Methodology, Investigation, Formal analysis, Data curation. **Chun-xiang Xu:** Supervision, Resources, Project administration. **Hong-zhen Lian:** Writing – review & editing, Supervision, Resources, Project administration, Funding acquisition, Conceptualization. **Jun-qin Qiao:** Validation, Methodology, Data curation. **Hui Lin:** Software, Resources, Investigation.

Declaration of Competing Interest

The authors declare that they have no known competing financial interests or personal relationships that could have appeared to influence the work reported in this paper.

Acknowledgments

This work was supported by the National Key R&D Program of China (No. 2019YFC1605400), and the National Natural Science Foundation of China (No. 22176085, No. 21874065).

Appendix A. Supporting information

Supplementary data associated with this article can be found in the online version at doi:10.1016/j.jhazmat.2025.137195.

Data availability

Data will be made available on request.

References

[1] Hong, S., Kwon, N., Kang, H., Jang, E., Kim, H., Han, E., 2022. Development of an analytical method for detection of anesthetics and sedatives in fish. J AOAC Int 105 (3), 774–783. https://doi.org/10.1093/jaoacint/qsab155.
[2] Kucharski, D., Nałęcz-Jawecki, G., Drzewicz, P., Skowronek, A., Mianowicz, K., Strzelecka, A., et al., 2022. The assessment of environmental risk related to the occurrence of pharmaceuticals in bottom sediments of the Odra River estuary (SW Baltic Sea). Sci Total Environ 828, 154446. https://doi.org/10.1016/j.scitotenv.2022.154446.
[3] Chang, X., Shen, Y., Yang, M., Yun, L., Liu, Z., Feng, S., et al., 2024. Antipsychotic drug-induced behavioral abnormalities in common carp: the potential involvement of the gut microbiota-brain axis. J Hazard Mater 472, 134444. https://doi.org/10.1016/j.jhazmat.2024.134444.
[4] Escudero, J., Muñoz, J.L., Morera-Herreras, T., Hernandez, R., Medrano, J., Domingo-Echaburu, S., et al., 2021. Antipsychotics as environmental pollutants: an underrated threat? Sci Total Environ 769, 144634. https://doi.org/10.1016/j.scitotenv.2020.144634.
[5] Wang, W., Wang, J., Wang, M., Shen, J., 2021. Rapid quantification of chlorpromazine residues in pork using nanosphere-based time-resolved fluorescence immunoassay analyzer. Int J Anal Chem 2021, 6633016. https://doi.org/10.1155/2021/6633016.
[6] Varak Neshin, M., Sanavi Khoshnood, R., Sanavi Khoshnoud, D., 2023. Surfactant assisted magnetic dispersive micro solid phase extraction-HPLC as a straightforward and green procedure for preconcentrating and determining Caffeine, Lidocaine, and Chlorpromazine in biological and water samples. Int J Environ Anal Chem 103 (20), 9661–9678. https://doi.org/10.1080/03067319.2021.2014473.
[7] Hoehns, J.D., Stanford, R.H., Geraets, D.R., Skelly, K.S., Lee, H., Gaul, B.L., 2001. Torsades de pointes associated with chlorpromazine: case report and review of associated ventricular arrhythmias. Pharmacotherapy 21 (7), 871–883. https://doi.org/10.1592/phco.21.9.871.34565.
[8] Vasquez, K.O., Peterson, J.D., 2017. Early detection of acute drug-induced liver injury in mice by noninvasive near-infrared fluorescence imaging. J Pharmacol Exp Ther 361 (1), 87–98. https://doi.org/10.1124/jpet.116.238378.
[9] European Union, 2005. Codex committee on resides of veterinary drugs in foods. Comments from the European Community on veterinary drugs without ADI/MRL.

[10] Ministry of Health, Labour and Welfare of Japan, 2005. Index of the positive list system for agricultural chemical residues in foods. G/SPS/N/JPN/145.

[11] National Standard of the People's Republic of China, 2019. National food safety standard - Maximum Residue Limits for Veterinary Drugs in Foods. GB 31650-2019.

[12] Ministry of Health, Labour and Welfare of Japan, 2016. Analytical Method for Chlorpromazine (Target to Animal and Fishery Products). ⟨https://www.mhlw.go.jp/stf/seisakunitsuite/bunya/kenkou_iryou/shokuhin/zanryu/index_00016.html⟩ (Accessed 2024.08.16).

[13] National Standard of the People's Republic of China, 2021. National food safety standard - Determination of chlorpromazine residue in fishery products by liquid chromatography-tandem mass spectrometric method. GB 31656, 4–2021.

[14] Fernández, C., González-Doncel, M., Pro, J., Carbonell, G., Tarazona, J.V., 2010. Occurrence of pharmaceutically active compounds in surface waters of the henares-jarama-tajo river system (madrid, spain) and a potential risk characterization. Sci Total Environ 408 (3), 543–551. https://doi.org/10.1016/j.scitotenv.2009.10.009.

[15] Roberts, P.H., Bersuder, P., 2006. Analysis of OSPAR priority pharmaceuticals using high-performance liquid chromatography-electrospray ionisation tandem mass spectrometry. J Chromatogr A 1134 (1-2), 143–150. https://doi.org/10.1016/j.chroma.2006.08.093.

[16] Yuan, S., Jiang, X., Xia, X., Zhang, H., Zheng, S., 2013. Detection, occurrence and fate of 22 psychiatric pharmaceuticals in psychiatric hospital and municipal wastewater treatment plants in Beijing, China. Chemosphere 90 (10), 2520–2525. https://doi.org/10.1016/j.chemosphere.2012.10.089.

[17] Reichert, J.F., Souza, D.M., Martins, A.F., 2019. Antipsychotic drugs in hospital wastewater and a preliminary risk assessment. Ecotoxicol Environ Saf 170, 559–567. https://doi.org/10.1016/j.ecoenv.2018.12.021.

[18] Richmond, E.K., Rosi, E.J., Walters, D.M., Fick, J., Hamilton, S.K., Brodin, T., et al., 2018. A diverse suite of pharmaceuticals contaminates stream and riparian food webs. Nat Commun 9, 4491. https://doi.org/10.1038/s41467-018-06822-w.

[19] Green, D.E., Forrest, I.S., 1966. *In vivo* metabolism of chlorpromazine. Can Psychiatr Assoc J 11 (4), 299–302. https://doi.org/10.1177/070674376601100405.

[20] Jiménez, J.J., Muñoz, B.E., Sánchez, M.I., Pardo, R., Vega, M.S., 2016. Fate of the drug chlorpromazine in river water according to laboratory assays. Identification and evolution over time of degradation products. Sorption to sediment. Chemosphere 162, 285–292. https://doi.org/10.1016/j.chemosphere.2016.07.107.

[21] Trautwein, C., Kümmerer, K., 2012. Degradation of the tricyclic antipsychotic drug chlorpromazine under environmental conditions, identification of its main aquatic biotic and abiotic transformation products by LC-MS^n and their effects on environmental bacteria. J Chromatogr B 889-890, 24–38. https://doi.org/10.1016/j.jchromb.2012.01.022.

[22] Nishimura, K., Okamura, N., Kimachi, T., Haginaka, J., 2019. Evaluation of molecularly imprinted polymers for chlorpromazine and bromopromazine prepared by multi-step swelling and polymerization method-The application for the determination of chlorpromazine and its metabolites in rat plasma by column-switching LC. J Pharm Biomed Anal 174, 248–255. https://doi.org/10.1016/j.jpba.2019.05.063.

[23] Dollery, C., Burley, D., 1991. Therapeutic Drugs. Churchill Livingstone, Edinburgh, pp. C201–C206. Vol. 1.

[24] Palumbo, F., Garcia-Lainez, G., Limones-Herrero, D., Coloma, M.D., Escobar, J., Jiménez, M.C., et al., 2016. Enhanced photo(geno)toxicity of demethylated chlorpromazine metabolites. Toxicol Appl Pharmacol 313, 131–137. https://doi.org/10.1016/j.taap.2016.10.024.

[25] Agúndez, J.A.G., García-Martín, E., García-Lainez, G., Miranda, M.A., Andreu, I., 2020. Photomutagenicity of chlorpromazine and its *N*-demethylated metabolites assessed by NGS. Sci Rep 10, 6879. https://doi.org/10.1038/s41598-020-63651-y.

[26] Dai, J., Lin, H., Pan, Y., Sun, Y., Wang, Y., Qiao, J., et al., 2023. Determination of chlorpromazine and its metabolites in animal-derived foods using QuEChERS-based extraction, EMR-Lipid cleanup, and UHPLC-Q-Orbitrap MS analysis. Food Chem 403, 134298. https://doi.org/10.1016/j.foodchem.2022.134298.

[27] Liang, C., Lian, H., 2015. Recent advances in lipophilicity measurement by reversed-phase high-performance liquid chromatography. Trends Anal Chem 68, 28–36. https://doi.org/10.1016/j.trac.2015.02.009.

[28] Han, S., Liang, C., Qiao, J., Lian, H., Ge, X., Chen, H., 2012. A novel evaluation method for extrapolated retention factor in determination of n-octanol/water partition coefficient of halogenated organic pollutants by reversed-phase high performance liquid chromatography. Anal Chim Acta 713, 130–135. https://doi.org/10.1016/j.aca.2011.11.020.

[29] Dai, J., Wang, Y., Lin, H., Sun, Y., Pan, Y., Qiao, J., et al., 2023. Residue screening and analysis of enrofloxacin and its metabolites in real aquatic products based on ultrahigh-performance liquid chromatography coupled with high resolution mass spectrometry. Food Chem 404, 134757. https://doi.org/10.1016/j.foodchem.2022.134757.

[30] National Standard of the People's Republic of China, 2006. Method for determination of acepromazine, chlorpromazine, haloperidol, propionylpromazine, xylazine, azaperone, azaperol and carazolol residues in porcine kidney and muscle tissues-LC-MS/MS method. GB/T 20763-2006.

[31] Professional Standard for Entry-Exit Inspection and Quarantine of the People's Republic of China, 2008. Determination of Residues of Tranquillizer Drugs in Animal-origin Foodstuffs for Import and Expert-LC-MS/MS Method. SN/T 2113-2008.

[32] Arimi, A., Dillert, R., Dräger, G., Bahnemann, D.W., 2019. Light-induced reactions of chlorpromazine in the presence of a heterogeneous photocatalyst: formation of a long-lasting sulfoxide. Catalysts 9 (7), 627. https://doi.org/10.3390/catal9070627.

[33] Wilde, M.L., Schneider, M., Kümmerer, K., 2017. Fenton process on single and mixture components of phenothiazine pharmaceuticals: assessment of intermediaries, fate, and preliminary ecotoxicity. Sci Total Environ 583, 36–52. https://doi.org/10.1016/j.scitotenv.2016.12.184.

[34] Campbell, C., Cornthwaite, H., Watterson, J., 2018. Oxidation of selected phenothiazine drugs during sample preparation: effects of varying extraction conditions on the extent of oxidation. J Anal Toxicol 42 (2), 99–114. https://doi.org/10.1093/jat/bkx067.

[35] Boehme, C.L., Strobel, H.W., 1998. High-performance liquid chromatographic methods for the analysis of haloperidol and chlorpromazine metabolism in vitro by purified cytochrome P450 isoforms. J Chromatogr B 718, 259–266. https://doi.org/10.1016/S0378-4347(98)00368-5.

[36] Silverman, R.B., Holladay, M.W., 2014. Drug Metabolism Chapter 8. The Organic Chemistry of Drug Design and Drug Action, Third ed. pp. 357-422.

[37] Tremaine, L.M., Welch, W.M., Ronfeld, R.A., 1989. Metabolism and disposition of the 5-hydroxytryptamine uptake blocker sertraline in the rat and dog. Drug Metab Dispos 17, 542–550.

[38] Cheng, W., Wang, X., Zhang, Z., Ma, L., Liu, G., Wang, Q., et al., 2021. Development of an isotope dilution UHPLC-QqQ-MS/MS-Based method for simultaneous determination of typical advanced glycation end products and acrylamide in baked and fried foods. J Agric Food Chem 69 (8), 2611–2618. https://doi.org/10.1021/acs.jafc.0c07575.

[39] Hartmann, N., Erbs, M., Wettstein, F.E., Hoerger, C.C., Schwarzenbach, R.P., Bucheli, T.D., 2008. Quantification of zearalenone in various solid agroenvironmental samples using D6-zearalenone as the internal standard. J Agric Food Chem 56 (9), 2926–2932. https://doi.org/10.1021/jf8002448.

[40] Medina-Pastor, P., Valverde, A., Pihlström, T., Masselter, S., Gamon, M., Mezcua, M., et al., 2011. Comparative study of the main top-down approaches for the estimation of measurement uncertainty in multiresidue analysis of pesticides in fruits and vegetables. J Agric Food Chem 59 (14), 7609–7619. https://doi.org/10.1021/jf104060h.

[41] ISO, 1993. Guide to the Expression of Uncertainty in Measurement. International Organization for Standardization, Geneva, Switzerland.

[42] Castillo, N.A., James, W.R., Santos, R.O., Rezek, R., Cerveny, D., Boucek, R.E., et al., 2024. Identifying pathways of pharmaceutical exposure in a mesoconsumer marine fish. J Hazard Mater 477, 135382. https://doi.org/10.1016/j.jhazmat.2024.135382.

[43] Dubreil, E., Sczubelek, L., Burkina, V., Zlabek, V., Sakalli, S., Zamaratskaia, G., et al., 2020. *In vitro* investigations of the metabolism of Victoria pure blue BO dye to identify main metabolites for food control in fish. Chemosphere 238, 124538. https://doi.org/10.1016/j.chemosphere.2019.124538.

[44] Ganorkar, S.B., Heyden, Y.V., 2022. Recent trends in pharmaceutical analysis to foster modern drug discovery by comparative *in-silico* profiling of drugs and related substances. TrAC-Trends Anal Chem 157, 116747. https://doi.org/10.1016/j.trac.2022.116747.

[45] A. Osawa, R., T. Barrocas, B., C. Monteiro, O., Oliveira, M.C., Florêncio, M.H., 2019. Photocatalytic degradation of cyclophosphamide and ifosfamide: effects of wastewater matrix, transformation products and *in silico* toxicity prediction. Sci Total Environ 692, 503–510. https://doi.org/10.1016/j.scitotenv.2019.07.247.

[46] Osawa, R.A., Barrocas, B.T., Monteiro, O.C., Conceição Oliveira, M., Florêncio, M.H., 2019. Photocatalytic degradation of amitriptyline, trazodone and venlafaxine using modified cobalt-titanate nanowires under UV-Vis radiation: transformation products and *in silico* toxicity. Chem Eng J 373, 1338–1347. https://doi.org/10.1016/j.cej.2019.05.137.

[47] Potęga, A., 2022. Glutathione-mediated conjugation of anticancer drugs: an overview of reaction mechanisms and biological significance for drug detoxification and bioactivation. Molecules 27 (16), 5252. https://doi.org/10.3390/molecules27165252.

[48] Fang, L., Xu, L., Zhang, N., Shi, Q., Shi, T., Ma, X., et al., 2021. Enantioselective degradation of the organophosphorus insecticide isocarbophos in *Cupriavidus nantongensis* X1^T: characteristics, enantioselective regulation, degradation pathways, and toxicity assessment. J Hazard Mater 417, 126024. https://doi.org/10.1016/j.jhazmat.2021.126024.

[49] EPA Toxicity Estimation Software Tool (TEST), 2022. ⟨https://www.epa.gov/chemical-research/toxicity-estimation-software-tool-test#history⟩ (Accessed 2023.11.29).

[50] Li, T., Zhou, Q., Zhang, N., Luo, Y., 2008. Toxic effects of chlorpromazine on Carassius auratus and its oxidative stress. J Environ Sci Health, Part B 43 (8), 638–643. https://doi.org/10.1080/03601230802352674.

[51] Sudeshna, G., Parimal, K., 2010. Multiple non-psychiatric effects of phenothiazines: a review. Eur J Pharmacol 648 (1-3), 6–14. https://doi.org/10.1016/j.ejphar.2010.08.045.

[52] Park, M., Lee, Y., Khan, A., Aleta, P., Cho, Y., Park, H., et al., 2019. Metabolite tracking to elucidate the effects of environmental pollutants. J Hazard Mater 376, 112–124. https://doi.org/10.1016/j.jhazmat.2019.05.024.

[53] Li, X., Zheng, S., Wu, G., 2020. Nutrition and metabolism of glutamate and glutamine in fish. Amino Acids 52 (5), 671–691. https://doi.org/10.1007/s00726-020-02851-2.

[54] Grillner, S., 2003. The motor infrastructure: from ion channels to neuronal networks. Nat Rev Neurosci 4 (7), 573–586. https://doi.org/10.1038/nrn1137.
[55] Wang, C., Qian, Y., Zhang, X., Chen, F., Zhang, Q., Li, Z., et al., 2016. A metabolomic study of fipronil for the anxiety-like behavior in zebrafish larvae at environmentally relevant levels. Environ Pollut 211, 252–258. https://doi.org/10.1016/j.envpol.2016.01.016.
[56] Oggier, D.M., Weisbrod, C.J., Stoller, A.M., Zenker, A.K., Fent, K., 2010. Effects of diazepam on gene expression and link to physiological effects in different life stages in Zebrafish *Danio rerio*. Environ Sci Technol 44 (19), 7685–7691. https://doi.org/10.1021/es100980r.